Published: 22 October 2025

Citation in BibTeX format

NANOCOM '25: 12th Annual ACM International Conference on Nanoscale Computing and Communication
October 23 - 25, 2025
Chengdu, China

RESEARCH-ARTICLE

Galvanic Coupling Channel Characterization for Wearable Devices

CHIARA CAVIGLIANO, Politecnico di Milano, Milan, MI, Italy

SILVIA MURA, Politecnico di Milano, Milan, MI, Italy

ANNA VIZZIELLO, University of Pavia, Pavia, PV, Italy

PIETRO SAVAZZI, University of Pavia, Pavia, PV, Italy

MAURIZIO MAGARINI, Politecnico di Milano, Milan, MI, Italy

NANOCOM '25: Proceedings of the 12th Annual ACM International Conference on Nanoscale Computing and Communication (October 2025)
https://doi.org/10.1145/3760544.3764132
ISBN: 9798400721663

Galvanic Coupling Channel Characterization for Wearable Devices

Chiara Cavigliano
DEIB, Politecnico di Milano
Milan, Italy
chiara.cavigliano@mail.polimi.it

Silvia Mura
DEIB, Politecnico di Milano
Milan, Italy
silvia.mura@polimi.it

Anna Vizziello
University of Pavia
Pavia, Italy
anna.vizziello@unipv.it

Pietro Savazzi
University of Pavia
Pavia, Italy
pietro.savazzi@unipv.it

Maurizio Magarini
DEIB, Politecnico di Milano
Milan, Italy
maurizio.magarini@polimi.it

Abstract

Galvanic Coupling (GC) Intra-Body Communication offers a promising solution for reliable, low-power data transmission in wearable medical devices. However, signal performance is highly sensitive to electrode material and skin–electrode interface properties. This study uses finite element modeling (FEM) to quantify the effects of electrode design, including material choice, conductive gel, and foam layers, on the GC channel frequency response (CFR), focusing on attenuation, phase delay, and group delay. Results show that incorporating gel and foam significantly enhances signal transmission by reducing attenuation, minimizing phase distortion, and stabilizing group delay across a broad frequency range. These improvements help mitigate performance disparities between Ag/AgCl and copper (Cu) electrodes, supporting the development of high-performance, energy-efficient intra-body networks for wearable healthcare applications.

Keywords

Intrabody Communications, Galvanic Coupling, COMSOL

ACM Reference Format:
Chiara Cavigliano, Silvia Mura, Anna Vizziello, Pietro Savazzi, and Maurizio Magarini. 2025. Galvanic Coupling Channel Characterization for Wearable Devices. In *International Conference on Nanoscale Computing and Communication (NanoCom '25), October 23–25, 2025, Chengdu, China.* ACM, New York, NY, USA, 6 pages. https://doi.org/10.1145/3760544.3764132

1 Introduction

With the rapid advancement of healthcare technology, wearable medical devices have become increasingly important for real-time monitoring and timely therapeutic interventions. These applications require highly reliable, low-latency communication systems. A foundational technology enabling such capabilities is the Intra-Body Network (IBN), which supports secure and efficient data exchange within the Internet of Medical Things (IoMT) and the Internet of Bio-Nano Things (IoBNT) [1].

NanoCom '25, Chengdu, China

ACM ISBN 979-8-4007-2166-3/25/10
https://doi.org/10.1145/3760544.3764132

At the core of IBNs lies Intra-Body Communication (IBC), which exploits the conductive properties of biological tissues to transmit data. IBC techniques can be broadly classified into mechanical, radio-frequency (RF), and electrical coupling methods [2]. Mechanical techniques, such as ultrasound, can reach deep tissues but suffer from high path loss and multipath effects. RF methods, including mmWave and THz, offer high data rates but are limited by rapid attenuation in water-rich tissues. In contrast, electrical coupling methods, namely Inductive Coupling (IC), Capacitive Coupling (CC), and Galvanic Coupling (GC), provide alternative solutions with varying trade-offs. IC relies on magnetic fields but is highly sensitive to coil alignment and distance. CC uses electric fields and requires an external ground reference, making it vulnerable to floating ground issues that hinder its use in wearable applications. GC, on the other hand, transmits differential currents through body tissues, offering localized signal propagation, minimal heating, and low power consumption, making it especially suitable for wearables [2].

GC-based IBC systems typically operate in the 10 kHz to 1 MHz range and are highly influenced by factors such as tissue composition, electrode placement, and electrode–skin interface characteristics. These include the use of conductive gels or foam layers, which play a critical role in signal injection and coupling efficiency [3]. To optimize GC communication and ensure robust IBN performance, a detailed understanding of the channel frequency response (CFR) is essential, specifically in terms of attenuation, phase delay, and group delay, which together govern signal loss, spectral distortion, and temporal alignment [1].

Experimental studies have explored how electrode design and interface properties influence IBC GC performance [4]. Pregelled Ag/AgCl electrodes typically offer low coupling resistance and improved signal injection, while solid-gel electrodes with foam backing (e.g., Blue Sensor BR, Neuroline 715) have been shown to reduce attenuation and support longer transmission distances, particularly across body segments like the upper arm and thorax [4]. Nonetheless, the GC CFR remains only partially characterized. While some trends are known, attenuation, phase delay, and group delay are not yet fully quantified, particularly across diverse operating conditions. Furthermore, experimental results are limited by subject variability and the heterogeneous structure of human tissues. Although controlled setups using muscle analogs and electrical phantoms

have been proposed [5], they often fail to capture the nuances of electrode–tissue interaction.

To bridge this gap, finite element modeling (FEM) has emerged as a powerful tool for simulating GC signal propagation in anatomically simplified body models. Prior work using FEM has examined factors like impedance variation, muscle conductivity, and posture-related effects [6, 7]. These studies have highlighted the dominant role of muscle in facilitating signal propagation, the attenuating effect exerted by the subcutaneous fat layer, and the decreasing attenuation of skin tissue with increasing frequency. However, existing models often oversimplify the electrode structure and omit key interface layers such as gel and foam, which are known to influence coupling and CFR characteristics. Notably, both simulations and in vivo studies [8] indicate that interface discontinuities can introduce nonlinear attenuation effects of up to 8 dB, underscoring the need for more accurate and complete electrode modeling.

Motivated by these limitations, this work investigates how electrode material and skin-electrode interface configuration impact the GC CFR. Specifically, we aim to quantify the effects of electrode design, including material, gel, and foam, on key CFR parameters: attenuation, phase delay, and group delay and analyze how these parameters vary across frequency. To this end, we perform FEM simulations in COMSOL Multiphysics [9], incorporating detailed electrode geometry and realistic interface layers. The results show that the combined use of conductive gel and foam substantially enhances signal transmission by lowering attenuation and phase delay while stabilizing group delay, effectively reducing signal distortion. Additionally, the joint use of gel and foam helps compensate for intrinsic differences between Ag/AgCl and Cu electrodes, particularly at low to mid frequencies, improving system reliability.

The rest of the paper is organized as follows: Section 2 introduces the system and channel model; Section 3 discusses critical electrode design aspects; Section 4 describes the simulation framework; Section 5 presents the numerical results; and Section 6 concludes the paper.

2 System and Channel Model

We consider the GC system illustrated in Fig. 1, comprising two electrode pairs placed on the surface of the human arm. Each electrode has a contact area A, with a longitudinal separation d_l between the transmitter (Tx) and receiver (Rx) pairs, and a radial spacing d_r within each pair.

A sinusoidal current $I_{\mathrm{TX}}(t) = I_0 \cos(\omega t + \phi_0)$ is applied across the Tx electrodes, where ω is the angular frequency and ϕ_0 is the phase offset. This current generates an electric field that propagates through body tissues, enabling galvanic signal transmission to the Rx electrodes. To comply with ICNIRP safety guidelines, the amplitude is limited to $I_0 \leq 1$mA.

Since body tissues act as a lossy and dispersive conductive medium, the injected current results in a voltage difference across the Tx electrodes, denoted as the transmitted differential voltage

$$\Delta V_{\mathrm{TX}}(\omega) = Z_{\mathrm{TX}}(\omega) \cdot I_{\mathrm{TX}}(\omega), \tag{1}$$

where $Z_{\mathrm{TX}}(\omega)$ is the complex impedance of the transmitter path, accounting for both tissue and electrode interface, including resistive and capacitive effects, and $I_{\mathrm{TX}}(\omega) = I_0 e^{j\phi_0}$ is the phasor of the input current. The voltage difference detected at the Rx electrodes

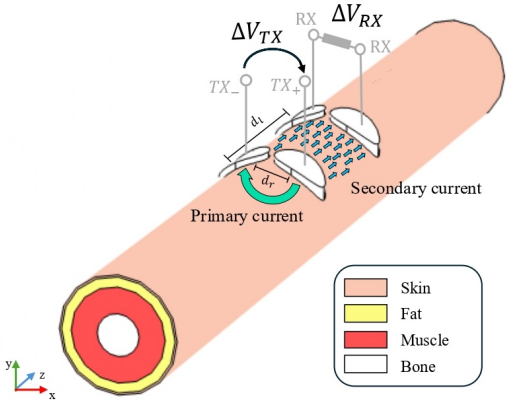

Fig. 1: GC system model based on a simplified concentric-layer arm model (skin, fat, muscle, bone).

is denoted as ΔV_{RX}, and the GC CFR, namely $H(\omega)$ is thus described by the transfer function

$$H(\omega) = \frac{\Delta V_{\mathrm{RX}}(\omega)}{\Delta V_{\mathrm{TX}}(\omega)} = \alpha(\omega)\ e^{-j\phi(\omega)}, \tag{2}$$

where $\alpha(\omega)$ represents the frequency-dependent attenuation magnitude, and $\phi(\omega)$ is the phase shift introduced by the channel.

In this study, the human arm is modeled as a concentric multi-layer cylinder with $N = 4$ anatomically relevant tissues: bone (core), muscle, subcutaneous fat, and skin (outermost), as shown in Fig.1. The frequency-dependent dielectric properties of each layer are defined using the Cole–Cole model [10], which accurately characterizes biological tissue permittivity from 10 Hz to 100 GHz. Assuming tissues are linear, isotropic, and homogeneous, the model accounts for multiple polarization mechanisms and ionic conductivity, yielding a realistic representation of dispersion in GC's operating range. The complex relative permittivity $\hat{\varepsilon}(\omega)$ is given by

$$\hat{\varepsilon}(\omega) = \varepsilon_\infty + \sum_{n=1}^{N} \frac{\Delta\varepsilon_n}{1 + (j\omega\tau_n)^{(1-\beta_n)}} + \frac{\sigma_i}{j\omega\varepsilon_0} \tag{3}$$

where: ε_∞ is the permittivity at infinite frequency, N is the number of dispersion regions, $\Delta\varepsilon_n$ is the magnitude of the nth dielectric dispersion, τ_n is the relaxation time of the nth dispersion process, β_n controls the broadening of each dispersion ($0 \leq \beta_n \leq 1$), σ_i is the static ionic conductivity and finally ε_0 is the vacuum permittivity.

The phase delay $\tau_d(\omega)$, quantifying the time it takes for a single-frequency (sinusoidal) component of the signal to travel from the Tx to the Rx, depends on the effective distance d_{eff} traveled by the signal as [11]

$$\tau_d(\omega) = \frac{d_{\mathrm{eff}}}{c} \sqrt{\Re\{\hat{\varepsilon}(\omega)\}}, \tag{4}$$

where c is the speed of light in vacuum and $\Re\{\cdot\}$ refers to real part operator. In dispersive biological tissues, phase delay varies with frequency due to the frequency-dependent dielectric properties of tissues. On the other hand, group delay $\tau_g(\omega)$ corresponds to the time delay experienced by the envelope of a modulated signal, and

it is defined as [12]

$$\tau_g(\omega) = -\frac{\delta(\phi(\omega))}{\delta\omega} = -\left[\tau_d(\omega) + \omega\,\frac{\delta(\tau_d(\omega))}{\delta\omega}\right]. \quad (5)$$

It expresses how rapidly the phase changes with frequency. In dispersive media like biological tissue, this delay is not constant, leading to signal distortion and dispersion.

The key parameters governing the GC-IBC channel, attenuation $\alpha(\omega)$, phase delay $\tau_p(\omega)$, and group delay $\tau_g(\omega)$, are influenced by both tissue properties (e.g., frequency-dependent conductivity and permittivity) and electrode characteristics. Electrode size, geometry, material, and the presence of intermediate layers (e.g., gel or foam) affect the electrode–tissue interface impedance, shaping signal coupling and propagation. Thus, optimizing GC-IBC performance requires careful electrode and interface design to minimize attenuation and distortion while preserving phase and timing accuracy.

3 Electrode Characteristics

The performance of GC IBC systems critically depends on electrode design and the electrode–skin interface, as factors such as shape, size, material, and configuration directly affect signal attenuation, phase delay, and group delay.

Previous studies have explored design trade-offs, e.g., larger electrodes reduce impedance but increase crosstalk, while smaller ones improve spatial resolution at the cost of higher impedance [13]; placement also influences signal path and noise [3]. To deepen the analysis, we investigate two widely used electrode types, Cu and Blue Sensor (Ag/AgCl-based) [4, 14], and systematically assess the role of interface materials (foam and gel), both separately and combined. Unlike prior work focused primarily on attenuation, our study evaluates the complete channel frequency response, including phase and group delay, offering a more comprehensive characterization of GC-IBC performance.

3.1 Copper and Bluesensors Electrodes

In GC systems, electrodes must balance electrical conductivity and biocompatibility to ensure reliable IBC. This study focuses on two representative types: copper and clinically used Blue Sensor electrodes. Cu is widely employed in simulations for its high conductivity, low cost, and modeling simplicity [15], though its susceptibility to oxidation and corrosion limits long-term biomedical use. Blue Sensor electrodes, commonly adopted in experiments [4, 14], use Ag/AgCl elements, offering good conductivity, biocompatibility, chemical stability, and antimicrobial properties, resulting in stable, low-impedance skin contact. Other materials, such as platinum and carbon-based electrodes, have been explored, but are excluded here due to limitations in cost, conductivity, or manufacturability. For these reasons, such alternatives are not considered in the present study.

3.2 Electrode Interface Materials

Biomedical and wearable electrodes often include a foam backing of medical-grade polyurethane or polyethylene for biocompatibility, flexibility, and hydrophilicity [4]. The foam, positioned as in Fig. 2, conforms to skin microtopography, ensuring stable contact,

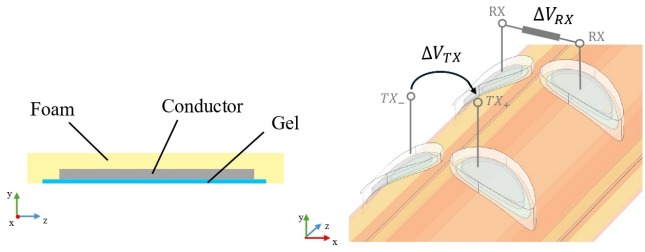

Fig. 2: Electrode structure and positioning: left shows layered components (foam, gel, conductor); right shows Tx/Rx pair configuration on the arm

reducing motion artifacts, and managing moisture by absorbing sweat to maintain consistent hydration and impedance. Sized to match the electrode area, it evenly distributes pressure, minimizes irritation, and enhances adhesion for long-term use [16].

Conductive gel, typically a hydrogel containing salts such as NaCl or KCl, reduces interface impedance and enhances electrical coupling [17], and is applied as shown in Fig. 2. It enables ion-to-electron transduction critical for stable signals and its viscosity balances coverage and spatial resolution, reducing cross-talk [18]. Though gel dehydration can raise impedance and degrade signals, foam helps retain moisture and electrochemical stability, ensuring reliable GC-IBC performance.

4 Finite Element Simulation Framework

This section outlines the simulation framework developed to characterize the CFR of GC-IBC under varying electrode and interface configurations. The analysis is conducted using FEM in COMSOL Multiphysics® [9], a platform for simulating coupled physical processes. The framework includes detailed models of the arm, electrodes, and interface modeling, enabling frequency-domain analysis of signal propagation. By capturing attenuation, phase delay, and group delay, it offers comprehensive insight into the impact of electrode and interface design on GC-IBC channel performance.

4.1 Arm Modeling

A 3D multilayer cylindrical model of the human arm is developed to simulate GC-based IBC, comprising $N = 4$ concentric tissue layers, skin, fat, muscle, and bone, arranged from outermost to innermost, as shown in Table 1. Each layer is assigned anatomically

Table 1: Geometric parameters of the multilayered cylindrical arm model [7].

Model Component	Value
Skin layer thickness	0.126 cm
Fat layer thickness	0.580 cm
Muscle layer thickness	1.550 cm
Bone layer thickness	1.244 cm
Arm external radius	3.5 cm
Arm length	60 cm
Air domain radius	600 cm
Electrode contact area	4 cm^2

Table 2: Cole-Cole parameters for selected biological tissues

Tissue type	ε_∞	$\Delta\varepsilon_1$	τ_1 (ps)	β_1	$\Delta\varepsilon_2$	τ_2 (ns)	β_2	$\Delta\varepsilon_3$	τ_3 (μs)	β_3	$\Delta\varepsilon_4$	τ_4 (ms)	β_4	σ
Bone	2.5	10.0	13.26	0.20	180	79.58	0.20	5.0×10^3	159.15	0.20	1.0×10^3	15.915	0.00	0.0200
Fat	2.5	3.0	7.96	0.20	15	15.92	0.10	3.3×10^4	159.15	0.05	1.0×10^7	7.958	0.01	0.0100
Muscle	4.0	50.0	7.23	0.10	7000	353.68	0.10	1.2×10^6	318.31	0.10	2.5×10^7	2.274	0.00	0.2000
Skin	4.0	32.0	7.23	0.00	1100	32.48	0.20	0.0	0.0	0.0	0.0	0.0	0.0	0.0002

Table 3: Geometric parameters of the electrode components

Component	Radius [cm]	Thickness [mm]
Conductor	$R_c = \sqrt{\frac{4}{\pi}}$	2.0
Foam	$R_f = R_c + 0.4$	3.7
Gel	$R_g = R_c + 0.2$	0.2

Table 4: Electrical properties of electrode and interface materials.

Material	Conductivity (S/m)	Relative Permittivity
Cu	5.998×10^7	1
Ag/AgCl	1.5×10^4	12
Conductive hydrogel	0.5	78
Foam backing	1×10^{-15}	1.5

and electrically representative properties based on Cole–Cole parameters in (3) from [10] (see Table 2), ensuring a physiologically accurate dielectric response across the frequency range relevant to IBC. To enable realistic field propagation and prevent non-physical reflections, the arm model is embedded within a spherical air domain, which acts as the surrounding medium and supports accurate boundary conditions. This setup allows for faithful simulation of electromagnetic field decay around the body. Surface-mounted circular electrodes are positioned on the skin layer to replicate galvanic coupling conditions. A constant contact area of $A = 4$ cm^2, representative of medium-sized electrodes commonly used in wearable GC systems, is adopted across all configurations to ensure fair comparison focused solely on the effects of electrode material and interface structure on signal transmission.

4.2 Electrodes and Interface Modeling

Two conductive materials, Cu and silver/silver chloride (Ag/AgCl), as detailed in Section 3, are considered for electrode modeling. Electrodes are circular, with geometric parameters reported in Table 3. To replicate realistic electrode–skin interactions, each conductor is paired with typical biomedical interface layers: a conductive hydrogel to enable low-resistance ionic coupling with the skin, and a foam backing for mechanical support and partial insulation. These layers are also circular, with dimensions listed in Table 3. A schematic representation of these electrode configurations is provided in Figure 2. The corresponding electrical properties, including conductivity and relative permittivity, are summarized in Table 4. This setup provides a controlled framework to assess how electrode materials and interface compositions influence signal transmission in GC-IBC systems.

4.3 Physics and Boundary Conditions

The simulation uses the *Electric Currents* module in COMSOL Multiphysics to solve the steady-state form of Maxwell's equations in conductive media, well-suited for GC-IBC where tissue conduction dominates. To approximate physiological continuity, *distributed impedance* boundary conditions are applied at the cylinder bases, enabling partial current flow and avoiding artificial reflections, thus emulating coupling with the torso without modeling the full body. The transmitter follows a unipolar excitation: one electrode injects a sinusoidal current ($I_0 = 1$ mA), while the other is grounded to complete the circuit [7]. Receiver electrodes are set with *floating potential* boundary conditions, mimicking passive sensing by high-impedance amplifiers. This configuration ensures that the measured voltage reflects the local conductive environment without influencing it [19].

5 Results and Discussion

This section presents simulation results based on the framework in Section 4, analyzing GC-IBC signal transmission over a frequency range of $10^4 - 10^6$ Hz. The setup uses fixed electrode geometry (d_l = 10 cm between Tx and Rx, d_r =3.5 cm within pairs) and compares two materials, Cu and silver/silver chloride (Ag/AgCl), across four interface configurations: bare, with foam, with hydrogel, and with both foam and hydrogel. The study evaluates how electrode material and interface composition affect CFT parameters, including signal attenuation, phase delay, and group delay.

The signal attenuation is evaluated in terms of signal gain between the Tx and Rx electrodes, computed based on the voltage ratio measured across the electrode pairs. The gain, expressed in decibels (dB), is defined as

$$G(\omega) = 20 \cdot \log_{10}\left(\frac{\Delta V_{\mathrm{RX}}}{\Delta V_{\mathrm{TX}}}\right) \tag{6}$$

where ΔV_{TX} and ΔV_{RX} denote the differential voltage amplitudes at the transmitter and receiver electrodes, respectively.

Fig. 3 presents the signal gain across frequency for different electrode configurations. At low to medium frequencies, bare Ag/AgCl electrodes exhibit the lowest gain (approximately −74 dB), while bare Cu electrodes show a moderately higher gain of about 2 dB, indicating reduced attenuation. The addition of a foam layer significantly improves the performance of Ag/AgCl electrodes, increasing gain by approximately 3 dB. In contrast, the foam layer has a negligible effect on Cu electrodes, whose performance remains comparable

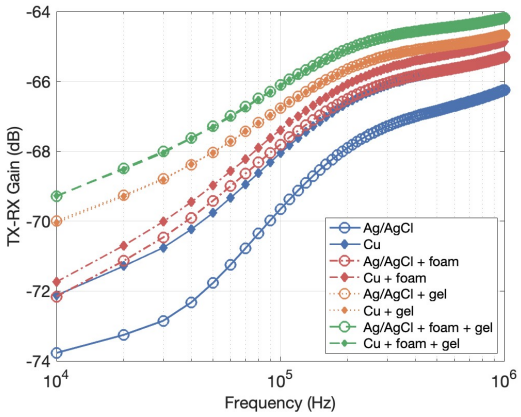

Fig. 3: Signal gain vs frequency across all electrode configurations.

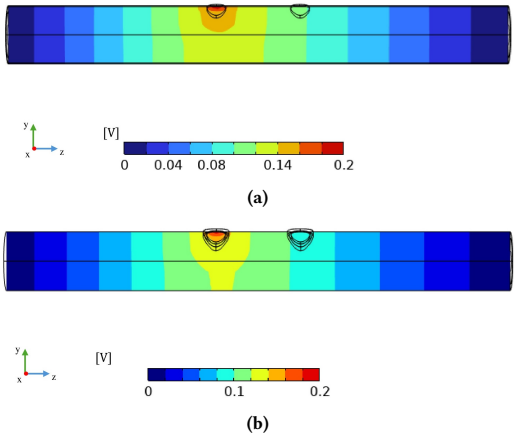

Fig. 4: Voltage distribution across different arm layers at 10^4 Hz for various electrode configurations, with the Tx electrode on the left and the Rx on the right: (a) bare Ag/AgCl electrode, (b) Ag/AgCl electrode with foam and conductive gel.

to the bare configuration. The application of conductive hydrogel alone yields a more pronounced enhancement, with gain improvements of around 4 dB for Ag/AgCl and 2 dB for Cu, indicating greater effectiveness with Ag/AgCl. The combined use of foam and gel results in the highest observed gains, improving Ag/AgCl by nearly 6 dB and Cu by approximately 4.5 dB compared to their bare counterparts. Under this configuration, both electrode types exhibit nearly identical gain, demonstrating that the combined use of foam and gel effectively compensates for intrinsic material differences and maximizes transmission efficiency. At higher frequencies, the relative gain differences diminish, and all configurations tend to converge in performance, indicating that the enhancements provided by foam and gel are primarily beneficial at lower and medium frequencies. It is important to note that, despite Cu's superior conductivity, it is not suitable for practical applications due to its susceptibility to oxidation. These results highlight that Ag/AgCl electrodes, although less conductive, can achieve comparable performance to Cu when used with both foam and gel, making them a more viable option for long-term biomedical applications. Additionally, Fig. 4 presents the voltage potential distribution across arm tissues for two configurations: the bare Ag/AgCl electrode and the Ag/AgCl electrode combined with foam and gel. In the bare Ag/AgCl case (Fig. 4a), voltage dispersion is greater, with more pronounced propagation into deeper tissue layers such as fat, muscle, and bone. In contrast, the foam-and-gel configuration exhibits reduced voltage penetration into these layers. This observation aligns with the gain analysis, supporting the conclusion that foam and gel mitigate signal attenuation by improving electrode–skin coupling.

Fig. 5 presents the phase delay across frequencies for various electrode configurations. At low frequencies, bare Cu and Ag/AgCl electrodes exhibit the highest phase delays, with minimal differences between the two materials. The addition of foam significantly reduces the phase delay for Ag/AgCl, by a factor of 4.5, but has a negligible effect on Cu. The application of conductive gel, both alone and in combination with foam, yields up to a fivefold reduction in phase delay for both Cu and Ag/AgCl compared to their bare counterparts. As frequency increases, phase delay rapidly decreases and converges across all configurations. This trend mirrors the attenuation behavior observed in Fig. 3, where differences among materials and configurations are more pronounced at low to medium frequencies but diminish at higher frequencies. Notably, the combined use of gel and foam is particularly beneficial for Ag/AgCl electrodes, significantly reducing phase delay and thereby enhancing end-to-end latency, minimizing phase distortion, and improving temporal synchronization, all critical requirements for IBC.

Finally, Fig. 6 shows the group delay across different electrode configurations. Higher or frequency-dependent group delay causes different frequency components to experience varying delays, leading to temporal smearing and signal distortion. At low frequencies, bare Ag/AgCl and Cu electrodes exhibit notably higher group delay,

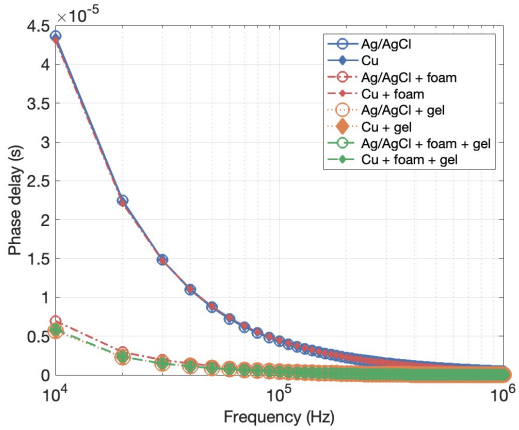

Fig. 5: Phase delay vs frequency across all electrode configurations.

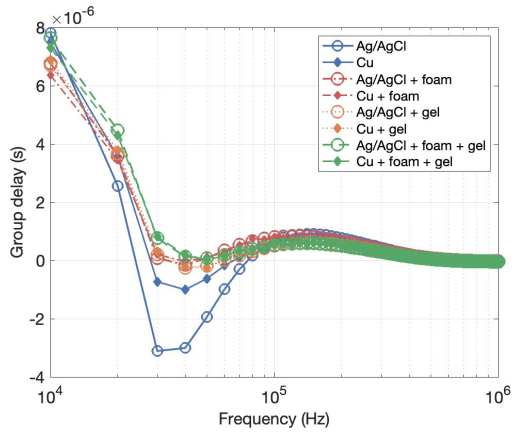

Fig. 6: Group delay vs frequency across all electrode configurations.

with negative group delay appearing near 20 kHz and 70 kHz, more pronounced in Ag/AgCl. These dispersion effects degrade communication performance and may reduce data rates and increase bit error rates. Negative group delay does not violate causality but indicates anomalous dispersion, where the system's phase response increases with frequency. This arises from resonant interactions in the complex impedance of tissue, electrodes, and interface materials like foam and gel, causing rapid phase shifts and phase advancement. Between 20 and 100 kHz, foam yields the lowest and most stable group delay, preventing negative delays and minimizing dispersion. Gel alone shows a slightly negative delay, while the gel-foam combination increases low-frequency delay compared to foam alone, but improves high-frequency performance above 100 kHz. These results emphasize the importance of interface materials in managing dispersion and optimizing signal integrity in GC channels.

In conclusion, the numerical results demonstrate that the combined use of conductive gel and foam significantly enhances signal transmission in GC channels by improving gain, reducing phase delay, and stabilizing group delay, thereby compensating for intrinsic material differences between Ag/AgCl and Cu electrodes. These improvements are most pronounced at low to medium frequencies and are critical for minimizing signal distortion, enhancing data rates, and ensuring reliable biomedical communication performance.

6 Conclusions

This study highlights the potential of GC for efficient and reliable IBC in medical systems. Leveraging on numerical simulations, we demonstrate that the use of conductive gel and foam interface layers can significantly improve signal transmission by reducing attenuation, minimizing phase distortion, and stabilizing group delay across a wide frequency range. These enhancements are also valuable for mitigating the performance differences between commonly used electrode materials, such as Ag/AgCl and Cu. The results support the feasibility of optimized electrode interface design as a key enabler for high-performance IBNs, paving the way for more robust and energy-efficient wearable device networks. Future work could extend the analysis beyond Cu and Ag/AgCl to alternative electrode materials, thereby further quantifying the impact of material properties and manufacturability. Additional studies may also assess long-term practicality, like gel dehydration and reusability, skin comfort, and end-to-end power consumption of GC-based IBC.

Acknowledgments

This study was partially supported by the European Union under the Italian National Recovery and Resilience Plan (NRRP) of NextGenerationEU, partnership on "Telecommunications of the Future" (PE00000001 - program "RESTART").

References

[1] David Naranjo-Hernández, Amparo Callejón-Leblic, Željka Lučev Vasić, MirHojjat Seyedi, and Yue-Ming Gao. Past results, present trends, and future challenges in intrabody communication. *Wireless communications and mobile computing*, 2018(1):9026847, 2018.

[2] Anna Vizziello, Maurizio Magarini, Pietro Savazzi, and Laura Galluccio. Intrabody communications for nervous system applications: Current technologies and future directions. *Computer Networks*, 227:109718, 2023.

[3] Marc Simon Wegmueller, Sonja Huclova, Juerg Froehlich, Michael Oberle, Norbert Felber, Niels Kuster, and Wolfgang Fichtner. Galvanic coupling enabling wireless implant communications. *IEEE Transactions on Instrumentation and Measurement*, 58(8):2618–2625, 2009.

[4] Robert Wegmüller, Markus Stager, Matthias Felder, Peter Boesiger, and Hans Ermert. Signal transmission by galvanic coupling through the human body. *IEEE Transactions on Instrumentation and Measurement*, 59(4):963–969, 2010.

[5] Anna Vizziello, Pietro Savazzi, Giovanni Magenes, and Paolo Gamba. Phy design and implementation of a galvanic coupling testbed for intra-body communication links. *IEEE Access*, 8:184585–184597, 2020.

[6] M. Amparo Callejón, P. del Campo, Javier Reina-Tosina, and Laura M. Roa. A parametric computational analysis into galvanic coupling intrabody communication. *IEEE Journal of Biomedical and Health Informatics*, 22(4):1087–1096, 2018.

[7] Doaa Ahmed, Georg Fischer, and Jens Kirchner. Simulation-based models of the galvanic coupling intra-body communication. In *2019 IEEE Sensors Applications Symposium (SAS)*, pages 1–6. IEEE, 2019.

[8] Marc Simon Wegmueller, Andreas Kuhn, Juerg Froehlich, Michael Oberle, Norbert Felber, Niels Kuster, and Wolfgang Fichtner. An attempt to model the human body as a communication channel. *IEEE transactions on Biomedical Engineering*, 54(10):1851–1857, 2007.

[9] COMSOL Multiphysics. Introduction to comsol multiphysics®. *COMSOL Multiphysics, Burlington, MA, accessed Feb*, 9(2018):32, 1998.

[10] Sami Gabriel, RW Lau, and Camelia Gabriel. The dielectric properties of biological tissues: Iii. parametric models for the dielectric spectrum of tissues. *Physics in medicine & biology*, 41(11):2271, 1996.

[11] Johan Sten and A Hujanen. Aspects on the phase delay and phase velocity in the electromagnetic near-field. *Progress In Electromagnetics Research*, 56:67–80, 2006.

[12] Bayya Yegnanarayana and Hema A Murthy. Significance of group delay functions in spectrum estimation. *IEEE Transactions on signal processing*, 40(9):2281–2289, 1992.

[13] Yu Ping Qin. Effect of electrode size on signal attenuation in intra-body communication. *Applied Mechanics and Materials*, 427:2029–2032, 2013.

[14] M Amparo Callejon, Javier Reina-Tosina, David Naranjo-Hernández, and Laura M Roa. Galvanic coupling transmission in intrabody communication: A finite element approach. *IEEE Transactions on Biomedical Engineering*, 61(3):775–783, 2013.

[15] Kayhan Ateş, Anna Marcucci, Pietro Savazzi, Şükrü Özen, Fabio Dell'Acqua, and Anna Vizziello. Channel characterization of implantable intrabody communication through experimental measurements. In *Proceedings of the 11th Annual ACM International Conference on Nanoscale Computing and Communication*, pages 66–71, 2024.

[16] Takuma Takagi, Naoto Tomita, Suguru Sato, Michitaka Yamamoto, Seiichi Takamatsu, and Toshihiro Itoh. Wearable emg measurement device using polyurethane foam for motion artifact suppression. *Sensors*, 24(10):2985, 2024.

[17] Sebastian R. Martinez, Paul LeFloch, Jia Liu, and Robert D. Howe. Pure conducting polymer hydrogels increase signal-to-noise of cutaneous electrodes by lowering skin interface impedance. *Advanced Healthcare Materials*, 12(17):e2202661, 2023.

[18] Yulin Fu, Jingjing Zhao, Ying Dong, and Xiaohao Wang. Dry electrodes for human bioelectrical signal monitoring. *Sensors*, 20(13):3651, 2020.

[19] Zhiying Chen, Yueming Gao, Min Du, and Feng Lin. A circuit-coupled fem model with considering parasitic capacitances effect for galvanic coupling intrabody communication. *Progress In Electromagnetics Research C*, 106:17–27, 2020.